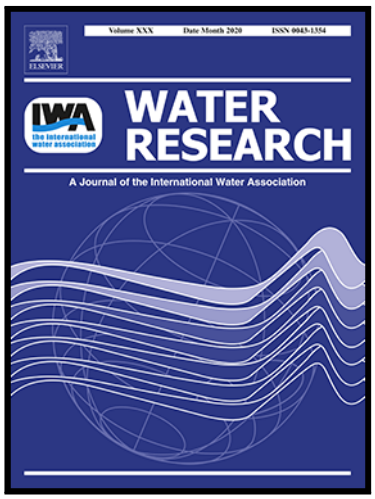

Nonlinear pattern and algal dual-impact in N_2O emission with increasing trophic levels in shallow lakes

Yiwen Zhou , Xiaoguang Xu , Kang Song , Senbati Yeerken , Ming Deng , Lu Li , Shohei Riya , Qilin Wang , Akihiko Terada

PII: S0043-1354(21)00687-4
DOI: https://doi.org/10.1016/j.watres.2021.117489
Reference: WR 117489

To appear in: *Water Research*

Received date: 24 February 2021
Revised date: 12 July 2021
Accepted date: 26 July 2021

Please cite this article as: Yiwen Zhou , Xiaoguang Xu , Kang Song , Senbati Yeerken , Ming Deng , Lu Li , Shohei Riya , Qilin Wang , Akihiko Terada , Nonlinear pattern and algal dual-impact in N_2O emission with increasing trophic levels in shallow lakes, *Water Research* (2021), doi: https://doi.org/10.1016/j.watres.2021.117489

Nonlinear pattern and algal dual-impact in N_2O emission with increasing trophic levels in shallow lakes

Yiwen Zhou[a,c,1], Xiaoguang Xu[b,1], Kang Song[a,d,*], Senbati Yeerken[a,d], Ming Deng[a], Lu Li[a], Shohei Riya[c], Qilin Wang[e], Akihiko Terada[c]

[a]State Key Laboratory of Freshwater Ecology and Biotechnology, Institute of Hydrobiology, Chinese Academy of Sciences, Wuhan 430072, China

[b]School of Environment, Nanjing Normal University, Nanjing 210023, China

[c]Department of Chemical Engineering, Tokyo University of Agriculture and Technology, Tokyo 184-8588, Japan

[d]University of Chinese Academy of Sciences, Beijing, China

[e]Centre for Technology in Water and Wastewater, School of Civil and Environmental Engineering, University of Technology Sydney, NSW 2007, Australia

[1]*Both authors contributed equally.*

**Corresponding author:*

No.7 Donghu South Road, Wuhan 430072, China; Email: sk@ihb.ac.cn (K. Song)

Highlights

- Net N_2O emissions from shallow lakes depend on eutrophication progress
- N_2O emissions of different lakes were distinguished by a nonlinear model
- Algal accumulation plays a dual role in regulating N_2O emissions
- N_2O emission fluxes were higher in winter than in summer in shallow lakes

- N_2O emissions in eutrophic lakes were overestimated by IPCC

Graphical Abstract

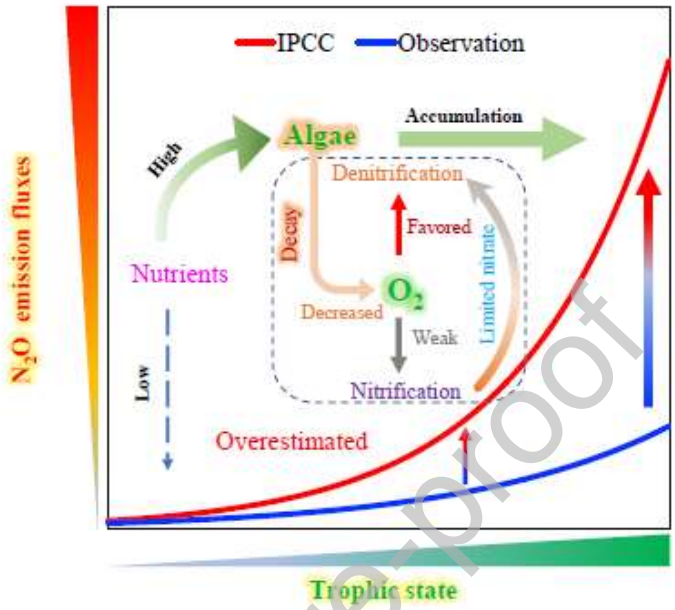

Abstract

Shallow lakes are considered important contributors to emissions of nitrous oxide (N_2O), a powerful greenhouse gas, in aquatic ecosystems. There is a large degree of uncertainty regarding the relationship between N_2O emissions and the progress of lake eutrophication, and the mechanisms underlying N_2O emissions are poorly understood. Here, N_2O emission fluxes and environmental variables in different lakes along a trophic state gradient in the Yangtze River basin were studied. N_2O emission fluxes were –1.0–53.0 μg m^{-2} h^{-1} and 0.4–102.9 μg m^{-2} h^{-1} in summer and winter, respectively, indicating that there was marked variation in N_2O emissions among lakes of different trophic state. The non-linear exponential model explained differences in N_2O emission

fluxes by the degree of eutrophication ($p < 0.01$). TN and chl-*a* both predicted 86% of the N_2O emission fluxes in shallow lakes. The predicted N_2O emission fluxes based on the IPCC EF_{5r} overestimated the observed fluxes, particularly those in hyper-eutrophic lakes. These findings demonstrated that nutrient-rich conditions and algal accumulation are key factors determining N_2O emission fluxes in shallow lakes. Furthermore, this study also revealed that temperature and algae accumulation-decomposition determine an N_2O emission flux in an intricate manner. A low temperature, *i.e.*, winter, limits algae growth and low oxygen consumption for algae decomposition. The environment leaves a high dissolved oxygen concentration, slowing down N_2O consumption as the final step of denitrification. In summer, with the oxygen consumed by excess algal decomposition, the N_2O production is limited by the complete denitrification as well as the limited substrate supply of nitrate by nitrification in hypoxic or anoxic conditions. Such cascading events explained the higher N_2O emission fluxes from shallow lakes in winter compared with summer. This trend was amplified in hyper-eutrophic shallow lakes after algal disappearance. Collectively, algal accumulation played a dual role in stimulating and impeding N_2O emissions, especially in hyper-eutrophic lakes. This study expands our knowledge of N_2O emissions from shallow lakes in which eutrophication is underway.

Keywords

Nitrous oxide, Biogeographic scale, Eutrophication, Functional gene, Algal

accumulation

1 Introduction

Nitrous oxide (N_2O) is an ozone-depleting and highly potent greenhouse gas (GHG) with a long half-life that contributes to global warming, in addition to carbon dioxide (CO_2) and methane (CH_4), in the stratosphere (Ravishankara et al., 2009). Atmospheric N_2O has increased by 20% from 1750 to 2018 and is steadily increasing at a rate of 0.2% per year (Tian et al., 2020). The IPCC reported that approximately 10% of anthropogenic N_2O sources are derived from freshwater and coastal marine systems (IPCC, 2013). Given that inland freshwater lakes are recipients of nutrients transported from terrestrial ecosystems to trigger uncertainty of GHG emissions (Wang et al., 2009; Zhou et al., 2020a), they function as N_2O hot spots where the high turnover of nitrogen (N) compounds. Hence, the N_2O emissions from aquatic ecosystems have received considerable attention (Beaulieu et al., 2011; Kortelainen et al., 2020). Although multiple factors such as nutrient composition, eutrophication, and temperature likely regulate N_2O emissions from freshwater lakes at regional and global scales, the dominant factors affecting N_2O emissions in freshwater lakes remain poorly understood (Kortelainen et al., 2020; Li et al., 2018; Yan et al., 2017). There is also a need to evaluate and quantify the N_2O emissions of freshwater lake ecosystems given that they are globally significant sources of N_2O (Lauerwald et al., 2019). Generally,

understanding the mechanisms underlying variation in N_2O emissions from freshwater lakes can aid the development of policies to address global warming.

N_2O is mainly produced by a by-product from nitrification and an intermediate from denitrification (Wenk et al., 2016). Of these multiple sources, denitrification is thought to be a main source of N_2O in aquatic ecosystems (Beaulieu et al., 2011; Li et al., 2019a; Salk and Ostrom, 2019). N_2O reduction, the final step of denitrification ($NO_3^- \rightarrow NO_2^- \rightarrow NO \rightarrow N_2O \rightarrow N_2$), is catalyzed by N_2O reductase, which is encoded by the *nos*Z gene (Yoon et al., 2016). Denitrification plays a critical role in determining N_2O emission fluxes, including whether aquatic ecosystems are N_2O sources or sinks. N_2O production is regulated by microbial community structure in aquatic ecosystems (Zhao et al., 2018; Zhao et al., 2019). Microbial community composition affects the amount of N_2O emissions, as some bacteria lack *nos*Z and nitrite reductase genes, which significantly contribute to N_2O consumption and production in natural ecosystems, respectively (Domeignoz-Horta et al., 2016). Among several environmental factors, nutrients, redox conditions, and temperature determine the microbial guilds involved in N_2O production and consumption (Hinshaw and Dahlgren, 2013; Xiao et al., 2019). Seasonal changes involve multiple environmental fluctuations that affect lacustrine microbial community structure (Song et al., 2012) and lead to uncertainty in the magnitude of N_2O emissions. N conversion rates and eutrophication progress are crucial for regulating final N forms (N_2 or N_2O) in aquatic ecosystems (Jiang et al., 2020; Salk

and Ostrom, 2019; Zhu et al., 2020). Such N conversions are dynamic and dependent on eutrophication progress (Li et al., 2018; Liikanen et al., 2003). There is thus a need to understand the microbial processes that regulate N_2O sources or sinks in lakes of different trophic state and determine spatial heterogeneity in N_2O emissions.

Shallow lakes receive massive amounts of nutrients from anthropogenic activities, which potentially lead to changes in lake trophic state (Zhou et al., 2020a; Zhou et al., 2019). GHG emissions from eutrophic shallow lakes have also been surveyed, and this work has shed light on differences in N_2O emission fluxes among shallow lakes of different trophic state. In these surveys, the commonly used default emission factor (EF_{5r}) by the IPCC has been used (Maavara et al., 2019), which results in either an underestimation or overestimation of the N_2O budgets in freshwater ecosystems of different trophic state (Zhang et al., 2020). For example, Xiao et al.(2019) indicated that the mean N_2O emission fluxes in the East and West zones of Lake Taihu (eutrophic and oligotrophic, respectively) were substantially different, which is partially caused by N flowing to the lake. In addition, N loadings regulate the distribution of denitrifying bacteria, which is often indicated by functional genes for N_2O production (*nirS* and *nirK*) and consumption (*nosZ*) (Huang et al., 2011; Zhao et al., 2018). High N flowing to eutrophic lakes increases algal growth, potentially enhancing N_2O emissions and N turnover rates (Yan et al., 2017; Zhu et al., 2020). However, the accumulation of algae alters the redox conditions favoring denitrification (Yan et al., 2017), and more severe

anoxic conditions limit the supply of nitrogen oxides generated by nitrification required for denitrification (Zhu et al., 2020); these observations impede our understanding of the role of algae in N_2O emissions. Such correlations in eutrophic and hypereutrophic lakes have been extensively investigated (Lauerwald et al., 2019; Xiao et al., 2019); however, shallow lakes have been poorly studied. In particular, no studies have compared N_2O emission fluxes among lakes of different trophic state (Salk and Ostrom, 2019). The trophic state of lakes leads to uncertainty in N_2O emission estimates (Kortelainen et al., 2020), yet the relationship between N_2O emission fluxes and the trophic state of lakes is not entirely decoupled. Studies of the N_2O emissions of lacustrine trophic states on a biogeographic scale could help enhance our understanding of their potential to act as sources of N_2O emissions.

Approximately 0.9% of China is covered with lakes. There are a total of 2,693 lakes (> 1.0 km^2), about one-third of which are shallow lakes located in the middle and lower reaches of the Yangtze River basin (Ma et al., 2011). To enhance our understanding of the relationship between N_2O emissions and eutrophication in shallow lakes in the Yangtze River basin, we characterized spatiotemporal variation in N_2O emission fluxes and its underlying mechanisms in 17 lakes along a trophic state gradient at a biogeographic scale. We constructed a model to predict the N_2O emission patterns in shallow lakes of different trophic state. The aims of this study were to (i) identify N_2O emission patterns in shallow lakes of different trophic state; (ii) characterize

differences in the main microorganisms and functional genes for N_2O emissions in the sediments in shallow lakes of different trophic state; (iii) evaluate the relationship between environmental variables and N_2O emissions to reveal the main drivers of N_2O emissions; and (iv) elucidate the role of algae on N_2O emissions in shallow lakes. The results of this study enhance our ability to accurately predict N_2O emission patterns from shallow lakes.

2 Material and methods

2.1 Field survey

2.1.1 Lakes of different trophic state

This study designated 17 sampling shallow lakes (< 7 m deep) in the middle and lower reaches of the Yangtze River basin. Lakes were sampled in the winter (November) of 2017 and summer (August and September) of 2018. Lake Taihu, Lake Guchenghu, Lake Chaohu, and Lake Donghu were sampled in winter 2017. Because river inflow affects the environmental conditions of lakes (Zhou et al., 2019), all sampling sites were located more than 1 km away from the mouth of inflow rivers. Based on the trophic level index (*TLI*) (see Supporting Materials for a description of how *TLI* was calculated), these lakes were classified into four trophic states: mesotrophic ($30 < TLI \leq 50$), eutrophic ($50 < TLI \leq 60$), middle-eutrophic ($60 < TLI \leq 70$), and hyper-eutrophic ($TLI > 70$) (Fig. 1) (Zhou et al., 2020b).

2.1.2 Heavy algae-accumulated and light algae-accumulated zones in Lake Taihu

Lake Taihu is a eutrophic lake that has experienced frequent and intensive cyanobacteria blooms since the 1980s (Qin et al., 2010). To characterize N_2O emission fluxes with or without algae accumulation, three typical zones (from west to east) in Lake Taihu, heavy algae-accumulated (Zone A and B), transitional (Zone C), and light algae-accumulated zones (Zone D), were studied (Fig. 1c). Sampling was conducted in summer (July) and winter (November) in 2019. The physicochemical parameters of the surface water and N_2O emission fluxes were investigated.

2.2 Sample collection and analysis

At each sampling event, vertical samples (*i.e.*, overlying water (20 cm below the water level), surface sediment (0–10 cm), and gas samples) were collected in triplicate. The *in situ* dissolved oxygen (DO), temperature, and pH were measured with DO, temperature, and pH probes (HQ3d, HACH, USA) on-site, respectively. To measure dissolved N_2 concentrations in summer, a water sample from a glass water sampler (1 L) was slowly drained from the bottom and transferred to a sample vial (12 mL) through a silicone tube with minimal turbulence. The silicone tube was placed in the bottom of the vial to avoid the ingress of atmospheric N_2. Next, 60 μL of saturated $HgCl_2$ solution (0.5% v/v final concentration) was added to the sample vial to inhibit microbial activity. These samples were stored in an ice cooler on-site and immediately transported to the

laboratory in a cooler at 4ºC. Water samples for chemical analyses, including total nitrogen (TN), total phosphorus (TP), NO_3^--N, NH_4^+-N, dissolved organic carbon (DOC), and chlorophyll-*a* (chl-*a*), were tested using previously described procedures (Zhou et al., 2019). Briefly, TN and TP were measured using an ultraviolet spectrophotometry method and an ammonium molybdate spectrophotometric method, respectively. NO_3^- and NH_4^+ concentrations were measured by a water flow analyzer (Auto Analyzer 3, Seal, Germany), and the DOC concentration was determined using an elemental analyzer (Flash EA 1112, CE Instruments, Italy). Chl-*a* was quantified by extraction in 95% ethanol and measuring the absorbance at 630, 645, 663, and 750 nm using a UV-vis spectrophotometer (UV-6100, Mapada, China).

2.3 Tested and calculated N_2O emission fluxes

N_2O emission flux was estimated by a floating static chamber (Cole et al., 2010; Gålfalk et al., 2013). The headspace gas was collected between 11:00 and 14:00 using three floating static chambers (size: 38.5 cm × 30.5 cm × 18.5 cm) following a previously described procedure (Zhou et al., 2019). During each gas sampling event, six gas samples were collected at 10-min intervals for 1 h via a static chamber. The gas chromatography (7890B Agilent) configuration described by Shaaban et al. (2018) was used to measure the N_2O concentration. The detailed methods for calculating N_2O emission fluxes are described in our previous study (Zhou et al., 2019). N_2O emission

flux estimated by the floating static chamber method was calculated using Eq. (1):

$$F = \frac{V}{A} \times \frac{\mathrm{d}C}{\mathrm{dt}}, \qquad (1)$$

where F is the N_2O emission flux (μg m^{-2} h^{-1}); V (m^3) and A (m^2) are the static chamber volume and surface area, respectively; and dC/dt is the time derivative of the N_2O concentration (μg m^{-3} h^{-1}).

2.4 Dissolved N_2 concentration and excess dissolved N_2 concentration

Dissolved N_2 was measured by a membrane inlet mass spectrometer system (MIMSS) with a probe inlet (HPR-40, Hiden Analytical Co.) using the N_2:Ar method described in a previous study (Chen et al., 2014). N_2:Ar ratios were calculated based on the quadrupole instrument signal (N_2 and Ar pressures at a detector) and calibrated using air-equilibrated water standards (Weiss, 1970). The dissolved N_2 concentrations of triplicate water samples were analyzed, and excess dissolved N_2 concentrations (ΔN_2) were calculated following previously described methods (Chen et al., 2014). ΔN_2 (μmol L^{-1}) was calculated using Eq. (2):

$$\Delta N_2 = N_{2\,(water)} - N_{2(eq)}, \qquad (2)$$

where $N_{2(water)}$ is the dissolved N_2 concentration in water measured by MIMSS, and $N_{2(eq)}$ is the concentration expected if the water were in equilibrium with the atmosphere. Both were estimated following previously described methods (Weiss, 1970; Weiss and Price, 1980).

2.5 Prediction of N_2O emission fluxes based on the IPCC model

A predictive model was used to determine the N_2O emission factor (EF_{5r}) as recommended in the IPCC-2019 guidelines. The dissolved N_2O concentration (μg-N L^{-1}) was estimated using Eq. (3):

$$N_2O\text{-}N = NO_3^-\text{-}N \times EF_{5r}, \qquad (3)$$

where EF_{5r} is 0.26% according to the IPCC-2019 default value (IPCC, 2019), and NO_3^--N (μg-N L^{-1}) represents the concentration measured in a water column. N_2O emission fluxes (F', μg m^{-2} h^{-1}) were calculated by the dissolved N_2O concentration using the two-layer model of diffusive gas exchange, which is given as Eq. (4)

$$F' = k \times (C_w - C_{eq}), \qquad (4)$$

where C_w, is obtained from Eq. 3 and is the dissolved N_2O concentration in water estimated by the EF_{5r}; C_{eq} is the N_2O concentration in water that is in equilibrium with the atmosphere at the *in situ* air pressure and temperature; k is the gas transfer coefficient (m d^{-1}) and was normalized to the Schmidt number of 600, as described in the Supporting Materials (Cole and Caraco, 1998).

2.6 DNA extraction, high-throughput sequencing, and real-time qPCR analysis

Biomass for the sediment microbial community analysis was collected from lakes of different trophic state. DNA was extracted from the collected biomass using the DNA Isolation Kit (MOBIO, USA) per the manufacturer's instructions. The concentration and

purity of DNA were measured using a microvolume UV-VIS spectrophotometer (NanoDrop^{TM} One^{C}, Thermo Fisher Scientific, USA), and the extracted DNA was stored at −20ºC before further analysis. 16S rRNA gene high-throughput sequencing was conducted using an Illumina MiSeq platform (Magigene Biotechnology Co. Ltd., Guangzhou, China). The primers used for high-throughput sequencing were modified 515F (5′-GTGYCAGCMGCCGCGGTAA-3′) and 806R (5′-GGACTACHVGGGTWTCTAAT-3′) targeting the V3 and V4 hypervariable regions of both bacterial and archaeal 16S rRNA genes (Zhou et al., 2020b). Given that the *nirK* and *nirS* genes and the *nosZ* gene encode enzymes for N_2O production and consumption in denitrification, respectively (Zhao et al., 2018), the abundances of these three genes were analyzed. 16S rRNA gene abundances were quantified by real-time quantitative PCR (qPCR) with reported primer sets (Table S3). The PCR conditions for the amplification of *nirK*, *nirS*, and *nosZ* were described in a previous study (Chen et al., 2017).

2.7 Statistical analysis

Statistical analyses were conducted using SPSS 19.0 (SPSS Inc., Chicago, USA). Significant differences among lakes were determined by one-way analysis of variance (ANOVA). The thresholds for statistically significant and highly statistically significant were $p < 0.05$ and $p < 0.01$ (two-tailed), respectively. The Kolmogorov-Smirnov test

was conducted to determine if the data were normally distributed. The built-in exponential model of Origin 2019 software (OriginLab Inc., USA) was carried out to assess the relationship between N_2O emission fluxes and *TLI*.

3 Results

3.1 *In situ* N_2O emission fluxes in lakes of different trophic state

The *TLI* of the examined lakes ranged from 44.0 to 69.7 and from 43.3 to 76.7 in the summer and winter, respectively (Fig. S1). The hyper-eutrophic sampling sites were not included in the winter dataset. Among these examined lakes, the ranges of N_2O emission fluxes were –1.0–53.0 μg m^{-2} h^{-1} and 0.4–102.9 μg m^{-2} h^{-1} in summer and winter, respectively, indicating a high degree of variation in N_2O emission fluxes (Table S1 and Fig. 2). In addition, all examined lakes were N_2O sources, with the exception of mesotrophic lakes in summer. The mean N_2O emission fluxes of the middle-eutrophic lakes in winter (50.4 μg m^{-2} h^{-1}) were higher than those of the hyper-eutrophic (39.1 μg m^{-2} h^{-1}) and middle-eutrophic (7.4 μg m^{-2} h^{-1}) lakes in summer (Table S1). Overall, the N_2O emission fluxes gradually increased as *TLI* increased (Fig. 2a).

The lacustrine N_2O emission fluxes in both winter and summer were positively correlated with *TLI* (Fig. 2a). The N_2O emission fluxes exponentially increased with the *TLI*s of the sampled lakes (adj. $R^2 = 0.85$, $p < 0.01$ in summer; adj. $R^2 = 0.63$, $p < 0.01$ in winter). There was a non-linear relationship between the net N_2O emission fluxes and

TLI (adj. R^2 = 0.36, $p < 0.01$) (Fig. 2b). The N_2O emission fluxes increased as the *TLI* of lakes increased, and the increase was more pronounced in hypertrophic lakes. In addition, N_2O emission fluxes were predicted based on the EF_{5r} [Equation (3)]. There was a nonlinear exponential relationship between the predicted N_2O emission fluxes and *TLI* (adj. R^2 = 0.80, $p < 0.01$) (Fig. 2b). These fluxes were higher than the observed values, especially in the hyper-eutrophic lakes in summer (*TLI* > 70) (Fig. S2).

3.2 Dissolved N_2 concentration in shallow lakes

Mean dissolved N_2 concentrations across all lakes in summer ranged from 403.3 μmol L^{-1} to 443.8 μmol L^{-1} and exhibited an unimodal relationship with *TLI* (Fig. 3a). Among these examined lakes, the lowest dissolved N_2 concentration was observed in hyper-eutrophic lakes. There was a significant unimodal relationship between the dissolved N_2 concentration and *TLI* ($p < 0.001$). The excess dissolved N_2 (ΔN_2), which was obtained by subtracting dissolved N_2 from the saturated concentration, was consistently positive (8.1–16.1 μmol L^{-1}) in summer, indicating N_2 oversaturation. The trend of N_2 oversaturation as a function of *TLI* was consistent with dissolved N_2 (Fig. 3).

3.3 Relationship between environmental factors and N_2O emission fluxes

The Pearson correlations between N_2O emission fluxes and environmental parameters of the overlying water were analyzed in different seasons (Table S4). The

N_2O emission fluxes were significantly and positively correlated with TN, NO_3^--N, and *TLI* ($p < 0.01$). The correlation between chl-*a* and N_2O emission fluxes varied seasonally, and the correlation was stronger in summer. ΔN_2 was negatively correlated with N_2O emission fluxes, TN, NO_3^--N, and chl-*a* in summer ($p < 0.05$). There was a negative correlation between DO concentrations and N_2O emission fluxes ($p < 0.05$) in summer, and this correlation was not observed in winter and over the entire year ($p > 0.05$) (Table S4). The overlying water DO was higher in winter (> 7 mg L^{-1}) than in summer (Fig. S1b). During the survey period, the temperature of the overlying water ranged from 9.5°C to 15.1°C and 27.1°C to 31.3°C in winter and summer, respectively (Fig. S1c). The temperature was negatively correlated with N_2O emission fluxes in both summer and winter ($p < 0.05$, Table S5). N_2O emission fluxes showed significant and positive linear correlations with TN (adj, $R^2 = 0.797$, $p < 0.01$ in winter; adj. $R^2 = 0.908$, $p < 0.01$ in summer), NO_3^--N (adj. $R^2 = 0.787$, $p < 0.01$ in winter; adj. $R^2 = 0.826$, $p < 0.01$ in summer), and NH_4^+-N (adj. $R^2 = 0.39$, $p = 0.039$ in winter; adj. $R^2 = 0.484$, $p = 0.01$ in summer) (Fig. 4). In addition, there was a significant negative linear correlation between *TLI* and the C:N ratio (adj. $R^2 = 0.649$, $p < 0.001$) (Fig. S3). There was a strong nonlinear correlation between N_2O emission fluxes and the C:N ratio (adj. $R^2 = 0.414$, $p < 0.001$) (Fig. S5).

A multiple stepwise regression model incorporating the physicochemical variables of the overlying water was established for N_2O emission fluxes (Table 1). The results

showed that TN and TP concentrations can predict N_2O emission fluxes in summer (adj. $R^2 = 0.94$, $p < 0.001$). TN ($t_1 = 10.80$) was more strongly positively correlated with N_2O emission fluxes than TP ($t_2 = 2.93$), which indicated that TN was an important parameter determining N_2O emission fluxes in summer. In addition, TN, chl-*a*, and NO_3^--N could jointly predict N_2O emission fluxes (adj. $R^2 = 0.96$, $p < 0.001$) in winter, demonstrating that both TN (6.11) and chl-*a* (–6.56) are important parameters determining N_2O emission fluxes in winter. TN (12.83) and chl-*a* (–4.07) were important variables predicting N_2O emission flux in lakes (adj. $R^2 = 0.86$, $p < 0.01$).

3.4 Microbial community structure and denitrifier abundances in lakes of different trophic state

Relative abundances of microbes were obtained at the phylum level in summer and winter (Fig. 5). Overall, the top 15 phyla made up more than 80% of microbial communities in all lake sediments. The following six phyla accounted for over 60% of the total population in summer: *Proteobacteria*, *Chloroflexi*, *Bacteroidetes*, *Acidobacteria*, *Verrucomicrobia,* and *Planctomycetes*; those in the winter were *Proteobacteria, Bacteroidetes, Acidobacteria, Nitrospirae, Planctomycetes,* and *Verrucomicrobia.* The most abundant phylum was *Proteobacteria*, which had relative abundances in hyper-eutrophic, middle-eutrophic, eutrophic, and mesotrophic lakes of 30.6–44.2%, 32.3–42.4%, 31.8–39.9%, and 32.0–46.4%, respectively. *Proteobacteria*

(26.4–43.4%) was also common in all lakes in winter. Among the six dominant phyla, the relative abundances of *Chloroflexi* were 2.8–5.7% in winter and 4.7–15.9% in summer; the relative abundances of *Nitrospirae* were 2.3–9.7% in winter and 0.1–4.1% in summer.

The *nirS* gene abundances in winter (0.66×10^7–3.67×10^7 copies g^{-1}-sediment) were lower than those in summer (2.70×10^7–7.62×10^8 copies g^{-1}-sediment) (Fig. S5). By contrast, no significant difference was observed for *nirK* gene abundances in winter (0.36×10^7–2.29×10^7 copies g^{-1}-sediment) and summer (0.06×10^7–2.06×10^7 copies g^{-1}-sediment). The *nirS*/*nirK* ratio was greater than 1, indicating that the *nirS*-type denitrifiers were consistently more abundant than *nirK*-type denitrifiers in these shallow lakes (Fig. 6a). The ratios were 9–48 times higher in summer than in winter. In addition, the *nirS*/*nirK* ratio increased as *TLI* increased in summer and winter ($p < 0.05$). *nirS*/*nirK* and N_2O emission fluxes were also positively correlated (Fig. S6a). The abundance of *nosZ*, which encodes an enzyme for N_2O consumption, varied from 0.31×10^7 copies g^{-1}-sediment to 2.88×10^7 copies g^{-1}-sediment in winter, which was lower than that in summer (0.53×10^7–7.02×10^7 copies g^{-1}-sediment) (Fig. S5). Variation in the ratios of (*nirK* + *nirS*)/*nosZ* was lower among the shallow lakes in winter (0.8–9.5) than in summer (2.9–12.3) (Fig. 6b). The ratio of (*nirK* + *nirS*)/*nosZ* was positively correlated with *TLI* ($p = 0.022$) and N_2O emission flux (Fig. S6b). Further analysis revealed the relationship between the spatial distribution of these denitrifying genes and

multiple environmental factors (Fig. 7). A redundancy analysis (RDA) showed that the first two axes explained 60.38% of the variation in the denitrifying genes. The samples of the examined lakes were well separated among the different seasons. The RDA between the denitrifying gene abundances and environmental parameters indicated that temperature was an important factor affecting gene abundances. Among the tested parameters, *nirS* and *nosZ* abundances were sensitive to temperature compared with *nirK*. The dissimilarity in the abundance of denitrifying genes in lakes of different trophic state was greater in summer than in winter. The abundance of *nirS* was positively correlated with *TLI*, and the abundance of *nosZ* was marginally correlated with *TLI*.

3.5 Characterization of N_2O emissions in the heavy algae-accumulated and light algae-accumulated zones in Lake Taihu

The N loading and chl-*a* concentrations were higher in the heavy algae-accumulated zones (Zones A and B) than in the light algae-accumulated zone (Zone D) (Table S2). The N_2O emissions fluxes were characterized in summer and winter in the two typical zones in Lake Taihu. The N_2O emission fluxes were significantly higher in the heavy algae-accumulated zones (Zones A and B) and transitional zone (Zone C) than in the light algae-accumulated zone (Zone D). The N_2O emission fluxes were location-dependent and varied from 42.16–136.63 μg m^{-2} h^{-1} in

the heavy algae-accumulated zones (Zones A and B), 21.35–31.89 μg m^{-2} h^{-1} in the transitional zone (Zone C), and 3.7–4.71 μg m^{-2} h^{-1} in the light algae-accumulated zone (Zone D) (Fig. 8). These fluxes in the algae-accumulated zones were significantly different in summer and winter ($p < 0.05$), and differences were not significant in Zone C ($p = 0.076$) and Zone D ($p = 0.677$). There was an exponential relationship between *TLI* and N_2O emission fluxes (Fig. S7) (adj. $R^2 = 0.55$, $p < 0.05$).

4 Discussion

4.1 Nonlinear N_2O emission patterns

Shallow lakes are potential sources of N_2O emissions and have been extensively studied (Kortelainen et al., 2020; Lauerwald et al., 2019; McCrackin and Elser, 2011). Previous studies have documented variation in N_2O emissions across lakes of different trophic state (Kortelainen et al., 2020; Salk and Ostrom, 2019); nevertheless, predicting N_2O emission fluxes from shallow lakes remains a challenge. This study showed that the net N_2O emission fluxes in lakes located in the Yangtze River basin, which spans 1000 km, displayed spatial and temporal heterogeneity determined by lake trophic state (Fig. 2). Consistent with previous studies (Salk and Ostrom, 2019; Xiao et al., 2019; Zhou et al., 2020a), these findings indicate that eutrophic lakes in the Yangtze River basin are sources of N_2O emissions. The patterns of N_2O emission fluxes in the shallow lakes were not completely consistent with the results of previous studies and depended

on eutrophication progress. The N_2O emission fluxes in the eutrophic and middle-eutrophic lakes (Table S1) were similar to the global median value of N_2O emission flux in lakes, whereas the mean N_2O emission flux in the hyper-eutrophic lakes was 8.7–11.2 times higher than the global median value (Hu et al., 2016). Shallow lakes in a mesotrophic state in summer were N_2O sinks (Fig. 2 and Table S1); these findings expand our knowledge regarding the prerequisites for freshwater lakes to act as either N_2O sinks or sources (Lauerwald et al., 2019). Our study underscores the significance of lake trophic state in determining N_2O emission fluxes, which is supported by the correlation between net N_2O emission flux and trophic state (Fig. 2a). Whether lakes of different trophic state act as N_2O sources or sinks can be predicted based on this correlation.

The major contribution of this study is the exponential model based on *TLI*, which could provide a robust means for quantifying lake trophic state; this model can be used to predict the N_2O emissions from lakes. This model represents an improvement over previous approaches for estimating N_2O emission fluxes because previous approaches do not consider differences in lake trophic state (Lauerwald et al., 2019). This model can be used to assess N_2O emission fluxes in shallow lakes of different trophic state. The N_2O emission fluxes and *TLI* were well fitted in summer (adj. R^2 = 0.85) and winter (adj. R^2 = 0.63). However, the coefficient of determination was low (adj. R^2 = 0.36) when all data (*i.e.*, summer and winter) were incorporated into the model, which is

likely explained by the large differences in N_2O emission fluxes in winter and summer (Fig. 2). Therefore, seasonal differences in N_2O emission fluxes in shallow lakes should also receive consideration (Kortelainen et al., 2019; Miao et al., 2020). Given the limited data on seasonal differences and the limited number of shallow lakes investigated, more data on N_2O emission fluxes are required to verify the credibility of the model.

4.2 Potential drivers of N_2O emissions

Our results revealed that reactive N accumulation plays a major role in regulating lake trophic state levels and the biological N cycle and promotes N_2O emissions via denitrification in shallow lakes. Degradation and metabolism were similar among shallow lakes despite variation in trophic state. *Proteobacteria* was identified as a predominant phylum based on the 16S rRNA gene analysis, and it was commonly detected in lakes of different trophic state (Fig. 5) (Li et al., 2019b); *Proteobacteria* might potentially contribute to degradation and metabolism (Huang et al., 2019). Previous studies have indicated that copiotrophic groups such as *Proteobacteria* and *Bacteroidetes* with high growth rates tend to thrive in nutrient-rich conditions (Fierer et al., 2012). The overlying water and sediments likely stored abundant nutrients that could be used by microorganisms in shallow lakes. In addition, nutrient abundance is an important factor affecting the microorganisms responsible for N conversion

(Saarenheimo et al., 2015; Zhang et al., 2019). The denitrifying genes varied greatly among the different trophic lakes and seasons (Figs. 6 and S5). These results suggest that denitrification is an important source of N_2O emissions in shallow eutrophic lakes, which is consistent with the results of previous studies (Beaulieu et al., 2011; Zhang et al., 2020). This is also confirmed by the stronger correlation of N_2O emission flux with NO_3^- than with NH_4^+ (Fig. 4) and the negative correlation between DO and N_2O emission fluxes (Table S4). The significant relationship between *TLI* and (*nirK* + *nirS*)/*nosZ* (p = 0.022), which indicates the relative abundance of N_2O producers relative to N_2O consumers, suggests that N_2O production may be greater than N_2O consumption in hyper-eutrophic lakes (Fig. 6b) (Zhao et al., 2018). Higher net N_2O emission fluxes were observed in hyper-eutrophic lakes because of their higher nutrient availability and (*nirK* + *nirS*)/*nosZ* (Kortelainen et al., 2020). These findings might explain the close relationship between lake trophic state and N_2O emission flux.

N availability drives eutrophication, and the subsequent accumulation of algae alters the redox conditions favoring denitrification (Yan et al., 2017; Zhu et al., 2020) and increases N_2O emissions in shallow lakes. In freshwater ecosystems, N loadings significantly contribute to N_2O emissions via denitrification (Kortelainen et al., 2020; Mulholland et al., 2008), which explains the high N_2O emission fluxes observed in eutrophic lakes when N loading was high (Figs. 2 and 4). A stepwise linear regression model indicated that TN and chl-*a* (algal density) are important parameters explaining

N_2O emissions (Table 1). Following algal accumulation, algal decay alters redox conditions and releases organic matter *in-situ* (Yan et al., 2017; Zhu et al., 2020). Moreover, algal blooms result in low DO concentrations and the accumulation of organic matter in hyper-eutrophic lakes (Yan et al., 2017; Zhou et al., 2020b; Zhu et al., 2020). For example, algal accumulation in Lake Taihu accounts for >50% of the organic matter (Xu et al., 2019). A C:N ratio lower than 8 indicates that organic matter is mainly derived from autochthonous inputs (Meyers, 1994; Yan et al., 2017). The negative correlation between C:N ratio and *TLI* (Fig. S3) indicates that algal accumulation and decomposition alter the physicochemical conditions in shallow lakes. Therefore, the contribution of algal decomposition should receive increased consideration when exploring the relationship between N_2O emission fluxes and chl-*a*. Our results indicated that N_2O emission fluxes and the C:N ratio were negatively correlated ($p < 0.001$) (Fig. S5). Algal decomposition results in oxygen consumption and thus a low DO concentration, which is favorable for denitrification (Zhu et al., 2020). This observation is consistent with the negative correlation between DO and chl-*a* (Tables S4 and S5). These findings might potentially explain the roles of decomposed algae in stimulating N_2O emissions via consumed oxygen in eutrophic shallow lakes.

Temperature is an important variable determining denitrifier abundance and structure in both seasons (Figs. 6 and 7); the effect of temperature was also manifested by the differences in N_2O emissions among seasons (Fig. 2). This pattern is similar to a

previous study of 87 boreal lakes in Finland showing that N_2O emissions peaked in winter (Kortelainen et al., 2020). Among enzymes responsible for denitrification, N_2O reductase is most sensitive to changes in temperature (Kortelainen et al., 2020; Veraart et al., 2011; Zhou et al., 2020c). Our previous study indicated that *nosZ* in N_2O-reducing bacteria is strongly related to temperature (Zhou et al., 2020c). In addition, N_2O reduction activity is inhibited by oxygen exposure, which increases N_2O emissions (Song et al., 2019). Low temperature increased the oxygen concentration (Fig. S1), and the relationship between the ratio of *nirS* to *nirK* with *TLI* varied in winter (slope: 0.08) and summer (slope: 1.11) ($p < 0.05$) (Fig. 6a). Given that the algae in lakes gradually declined in winter concomitant with increasing DO concentrations (Fig. S1 and Table S1), N_2O emission fluxes in lakes increased in winter (Fig. 2a) (Miao et al., 2020). In summer, algal decay further decreased the oxygen concentration. Previous studies have shown that *nirK* only achieves high abundances in conditionally oxygen-exposed environment (Huang et al., 2011), whereas *nirS* genes have been more commonly detected in anoxic locations (Knapp et al., 2009). The observation that the N_2O emission fluxes, *nirS*/*nirK*, and (*nirS*+*nirK*)/*nosZ* showed more significant positive relationships in winter than in summer suggests that the N_2O emission fluxes in summer were also affected by other factors (Fig. S6). The dramatic difference between hyper-eutrophic lakes in winter and summer was in the frequency of algal blooms in hyper-eutrophic lakes in summer. The algae regulating N_2O emission fluxes in shallow lakes are

discussed in the subsequent section. In sum, low temperature associated with abundant N favored N_2O accumulation via control oxygen concentrations and limit N_2O reduction activity.

4.3 Dual impact of algae on N_2O emissions

N_2O emissions were highest, and the chl-*a* concentration low, in Zone B in contrast to Zone A in a heavy algae-accumulated zone of Lake Taihu (Fig. 8 and Table S2). This result is inconsistent with the finding that algal accumulation, reflected by *TLI*, stimulated N_2O emissions in a non-linear exponential manner in the other tested lakes (Fig. S7). In heavy algae-accumulated zones, lower N_2O emissions, indicated by the high chl-*a* concentration, likely stem from algal accumulation, which suppresses denitrification activities caused by the decrease in N_2O production. Recently, Zhu et al. (2020) reported that algal accumulation may inhibit denitrification during algal blooms in summer. Consistent with this finding, a unimodal relationship between *TLI* and excess dissolved N_2 (ΔN_2) in summer was observed (Fig. 3b), which indicated higher complete denitrification (*i.e.*, including N_2O consumption) rates in the eutrophic lakes (Chen et al., 2014; Wang et al., 2018). In summer, the highest gene abundances of *nirK*, *nirS*, and *nosZ* were observed in eutrophic and middle-eutrophic lakes rather than in hyper-eutrophic lakes (Fig. S5). Although more abundant N is available in hyper-eutrophic lakes, the complete denitrification rates may be lower in

hyper-eutrophic lakes than in eutrophic lakes in summer. This pattern potentially stems from the abundance of algal biomass in the hyper-eutrophic lakes, as release of algal debris eventually leads to reductive conditions (Table S2). The decay of excess algal biomass could create favorable conditions for denitrification where organic carbon is present under hypoxic or anoxic conditions. However, hypoxia limits nitrification, which leads to a deficiency in the supply of NO_3^- for denitrification (Small et al., 2014; Zhu et al., 2020). This effect is supported by previous work in zones with accumulated algae in Lake Taihu showing that the NH_4^+ concentration in sediments is two or three orders of magnitude higher than the NO_3^- concentration (Yan et al., 2019). Our results are also consistent with this observation (Table S2). In addition, chl-*a* (as a negative factor) and TN together predicted the N_2O emission fluxes (Table 1). Algal accumulation and decomposition create hypoxic conditions that limit nitrification by converting NH_4^+ into NO_3^-, eventually suppressing the ensuing denitrification. In addition, hypoxic conditions favor complete denitrifying bacteria for mitigating N_2O emissions. These results further explain why higher N_2O emission fluxes of shallow lakes were observed in winter rather than in summer (Figs. 2a and 8). Therefore, these evidences indicated that algal accumulation played a dual role in stimulating and impeding N_2O emissions, especially in hyper-eutrophic lakes.

4.4 Implications of eutrophication progress on N_2O emissions

In aquatic ecosystems, excessive N loadings drive eutrophication and promote N_2O emissions in water bodies (Zhao et al., 2015). Meanwhile, the nutrient overload induces algae growth in shallow lakes, forming an anoxic or microaerobic micro-environment favoring N_2O production by algae accumulation (Zhu et al., 2020). In this study, a nonlinear exponential increase in N_2O emission flux as a function of *TLI* in shallow lakes of different trophic state was observed (Fig. 2). Eutrophic lakes had high N_2O emission fluxes, which is consistent with the relationship between lake trophic state and CH_4 emission fluxes (Zhou et al., 2020b). The common trends indicate that increases in GHG emissions stem from eutrophication. The predicted N_2O emission fluxes based on the IPCC EF_{5r} overestimated the observed fluxes but also exhibited a non-linear exponential increase with *TLI* (Fig. 2b). Xiao et al. (2019) reported that the N_2O emission factor in Lake Taihu was 0.18%, which is lower than the value of EF_{5r} based on the reported IPCC value. The overestimation by the IPCC default value indicates the need to calibrate an N_2O emission factor in shallow lakes depending on the eutrophic state. Pronounced differences between the predicted and observed N_2O emission fluxes were observed in hyper-eutrophic lakes where the abundance of algae impeded N_2O emissions. The high abundance of algae in summer compared with winter indicates that the degree to which N_2O emission flux was overestimated in summer was different from that in winter (Fig. S2). Algal decomposition made the redox conditions favorable for denitrification but unfavorable for nitrification because of an insufficient supply of

NO_3^-. The retained nitrogen is absorbed by the newly grown algae (Zhu et al., 2020). In non-limited N, algal decay leads to low-oxygen conditions, which enhances denitrification and further stimulates N_2O emissions. Therefore, algae should be considered a nitrogen "pool" that maintains nitrogen in lakes. In such situations where algae pools N, lower N_2O emissions stemming from the suppression of nitrification do not contribute to the reduction in global N_2O emissions from lakes but potentially leads to substantial N_2O emissions from hyper-eutrophic state lakes when conditions for nitrification are suitable. We suggest that overestimation was possibly caused by the "dual role" of the algae because they help re-regulate denitrification to mitigate N_2O emissions. Estimation of flux by the two-layer model was one order of magnitude lower than that estimated by static chamber methods (Duchemin et al., 1999). Given that the two different methods plausibly overestimated or underestimated the N_2O emission fluxes in shallow lakes, an intensive survey of an N_2O emission factor in hyper-eutrophic lakes will be conducted in a follow-up study.

5 Conclusions

We performed a series of field measurements and characterized the N_2O emissions in shallow lakes of different trophic state in the Yangtze River basin. The results of this study are detailed below.

- The N_2O emission fluxes of shallow lakes were most strongly affected by lake

trophic state, suggesting that estimation of N_2O emission fluxes should consider lake trophic state.

- The nonlinear model incorporating trophic state levels can describe the N_2O emissions from a shallow lake.
- The predicted N_2O emission fluxes based on the IPCC EF_{5r} overestimated the observed fluxes, particularly those in hyper-eutrophic lakes.
- Nutrient-rich conditions and algal accumulation were key factors determining N_2O emission fluxes in shallow lakes, and algal accumulation played a dual role in stimulating and impeding N_2O emissions, especially in hyper-eutrophic lakes.
- Changes in season accompanied the appearance and disappearance of algae and altered N_2O emission fluxes, especially in hyper-eutrophic lakes.

Declaration of Competing Interests

The authors declare that they have no known competing financial interests or personal relationships that could have appeared to influence the work reported in this paper.

Acknowledgments

This work was supported by the National Natural Science Foundation of China (41877344 and 42077294), the 100 Talents Program of Chinese Academy of Sciences (E029040201, E051040101), the National Water Science and Technology Project (2018ZX07208001), the China Scholarship Council (CSC201808420224), the

Australian Research Council Future Fellowship (FT200100264), and TAMAGO (Technologically Advanced research through Marriage of Agriculture and engineering as Ground-breaking Organization) at Tokyo University of Agriculture and Technology. We thank the editor and anonymous reviewers for providing valuable comments on the manuscript.

References

Beaulieu, J.J., Tank, J.L., Hamilton, S.K., Wollheim, W.M., Hall, R.O., Jr., Mulholland, P.J., Peterson, B.J., Ashkenas, L.R., Cooper, L.W., Dahm, C.N., Dodds, W.K., Grimm, N.B., Johnson, S.L., McDowell, W.H., Poole, G.C., Valett, H.M., Arango, C.P., Bernot, M.J., Burgin, A.J., Crenshaw, C.L., Helton, A.M., Johnson, L.T., O'Brien, J.M., Potter, J.D., Sheibley, R.W., Sobota, D.J., Thomas, S.M., 2011. Nitrous oxide emission from denitrification in stream and river networks. Proceedings of the National Academy of Sciences of the United States of America 108, 214-219.

Chen, N., Chen, Z., Wu, Y., Hu, A., 2014. Understanding gaseous nitrogen removal through direct measurement of dissolved N_2 and N_2O in a subtropical river-reservoir system. Ecological Engineering 70, 56-67.

Chen, R., Deng, M., He, X., Hou, J., 2017. Enhancing nitrate removal from freshwater pond by regulating carbon/nitrogen ratio. Frontiers in Microbiology 8, 1712.

Cole, J.J., Bade, D.L., Bastviken, D., Pace, M.L., Van de Bogert, M., 2010. Multiple approaches to estimating air-water gas exchange in small lakes. Limnology and Oceanography: Methods 8, 285-293.

Cole, J.J., Caraco, N.F., 1998. Atmospheric exchange of carbon dioxide in a low-wind oligotrophic lake measured by the addition of SF6. Limnology and Oceanography 43, 647-656.

Domeignoz-Horta, L.A., Putz, M., Spor, A., Bru, D., Breuil, M.C., Hallin, S., Philippot, L., 2016. Non-denitrifying nitrous oxide-reducing bacteria - An effective N_2O sink in soil. Soil Biology and Biochemistry 103, 376-379.

Duchemin, E., Lucotte, M., Canuel, R., 1999. Comparison of static chamber and thin boundary layer equation methods for measuring greenhouse gas emissions from large water bodies. Environmental Science & Technology 33, 350-357.

Fierer, N., Lauber, C.L., Ramirez, K.S., Zaneveld, J., Bradford, M.A., Knight, R., 2012. Comparative metagenomic, phylogenetic and physiological analyses of soil microbial communities across nitrogen gradients. ISME Journal 6, 1007-1017.

Gålfalk, M., Bastviken, D., Fredriksson, S., Arneborg, L., 2013. Determination of the piston velocity for water-air interfaces using flux chambers, acoustic Doppler velocimetry, and IR imaging of the water surface. Journal of Geophysical Research: Biogeosciences 118, 770-782.

Hinshaw, S.E., Dahlgren, R.A., 2013. Dissolved nitrous oxide concentrations and fluxes from the eutrophic San Joaquin River, California. Environmental Science & Technology 47, 1313-1322.

Hu, M., Chen, D., Dahlgren, R.A., 2016. Modeling nitrous oxide emission from rivers: a global assessment. Global Change Biology 22, 3566-3582.

Huang, S., Chen, C., Yang, X., Wu, Q., Zhang, R., 2011. Distribution of typical denitrifying functional genes and diversity of the *nir*S-encoding bacterial community related to environmental characteristics of river sediments. Biogeosciences 8, 3041-3051.

Huang, W., Chen, X., Wang, K., Chen, J., Zheng, B., Jiang, X., 2019. Comparison among the microbial communities in the lake, lake wetland, and estuary sediments of a plain river network. Microbiologyopen 8, e00644.

IPCC In: Stocker T.F. et al (Eds)., 2013. Climate change 2013: the physical science basis. Contribution of working group I to the fifth assessment report of the Intergovernmental Panel on Climate Change. Cambridge University Press, New York. Cambridge University Press, New York.

IPCC, In: Calvo, Buendia, E.; Tanabe, K.; Kranjc, A.; Baasansuren, J.; Fukuda, M.; Ngarize, S.; Osako, A.; Pyrozhenko, Y.; Shermanau, P.; Federici, S.; (Eds.), 2019. Refinement to the 2006 IPCC guidelines for national greenhouse gas inventories, Volum 4. IPCC, Switzerland, Kanagawa, JAPAN. Chapter 11.

Jiang, X., Gao, G., Zhang, L., Tang, X., Shao, K., Hu, Y., Cai, J., 2020. Role of algal accumulations on the partitioning between N_2 production and dissimilatory nitrate reduction to ammonium in eutrophic lakes. Water Research 183, 116075.

Knapp, C.W., Dodds, W.K., Wilson, K.C., O'Brien, J.M., Graham, D.W., 2009. Spatial heterogeneity of denitrification genes in a highly homogenous urban stream. Environmental Science & Technology 43, 4273-4279.

Kortelainen, P., Larmola, T., Rantakari, M., Juutinen, S., Alm, J., Martikainen, P.J., 2020. Lakes as nitrous oxide sources in the boreal landscape. Global Change Biology 26, 1432-1445.

Lauerwald, R., Regnier, P., Figueiredo, V., Enrich-Prast, A., Bastviken, D., Lehner, B., Maavara, T., Raymond, P., 2019. Natural Lakes are a minor global source of N_2O to the atmosphere. Global Biogeochemical Cycles 33, 1564-1581.

Li, Q., Wang, F., Yu, Q., Yan, W., Li, X., Lv, S., 2019a. Dominance of nitrous oxide production by nitrification and denitrification in the shallow Chaohu Lake, Eastern China: Insight from isotopic characteristics of dissolved nitrous oxide. Environmental Pollution 255, 113212.

Li, S., Bush, R.T., Santos, I.R., Zhang, Q., Song, K., Mao, R., Wen, Z., Lu, X.X., 2018. Large greenhouse gases emissions from China's lakes and reservoirs. Water Research 147, 13-24.

Li, Y., Sun, Y., Zhang, H., Wang, L., Zhang, W., Niu, L., Wang, P., Wang, C., 2019b. The responses of bacterial community and N_2O emission to nitrogen input in lake sediment: Estrogen as a co-pollutant. Environmental Research 179, 108769.

Liikanen, A., Huttunen, J.T., Murtoniemi, T., Tanskanen, H., Vaisanen, T., Silvola, J., Alm, J., Martikainen, P.J., 2003. Spatial and seasonal variation in greenhouse gas and nutrient dynamics and their interactions in the sediments of a boreal eutrophic lake. Biogeochemistry 65, 83-103.

Ma, R., Yang, G., Duan, H., Jiang, J., Wang, S., Feng, X., Li, A., Kong, F., Xue, B., Wu, J., Li, S., 2011.

China's lakes at present: Number, area and spatial distribution. Science China Earth Sciences 54, 283-289.

Maavara, T., Lauerwald, R., Laruelle, G.G., Akbarzadeh, Z., Bouskill, N.J., Van Cappellen, P., Regnier, P., 2019. Nitrous oxide emissions from inland waters: Are IPCC estimates too high? Global Change Biology 25, 473-488.

McCrackin, M.L., Elser, J.J., 2011. Greenhouse gas dynamics in lakes receiving atmospheric nitrogen deposition. Global Biogeochemical Cycles 25, 1-12.

Meyers, P.A., 1994. Preservation of elemental and isotopic source identification of sedimentary organic matter. Chemical Geology 114, 289-302.

Miao, Y., Huang, J., Duan, H., Meng, H., Wang, Z., Qi, T., Wu, Q.L., 2020. Spatial and seasonal Variability of nitrous oxide in a large freshwater lake in the lower reaches of the Yangtze River, China. Science of Total Environment 721, 137716.

Mulholland, P.J., Helton, A.M., Poole, G.C., Hall, R.O., Hamilton, S.K., Peterson, B.J., Tank, J.L., Ashkenas, L.R., Cooper, L.W., Dahm, C.N., 2008. Stream denitrification across biomes and its response to anthropogenic nitrate loading. Nature 452, 202-205.

Qin, B., Zhu, G., Gao, G., Zhang, Y., Wei, L., Paerl, H.W., Carmichael, W.W., 2010. A drinking water crisis in Lake Taihu, China: Linkage to climatic variability and lake management. Environmental Management 45, 105-112.

Ravishankara, A.R., Daniel, J.S., Portmann, R.W., 2009. Nitrous oxide (N_2O): the dominant ozone-depleting substance emitted in the 21st century. Science 326, 123-125.

Saarenheimo, J., Tiirola, M.A., Rissanen, A.J., 2015. Functional gene pyrosequencing reveals core proteobacterial denitrifiers in boreal lakes. Frontiers in Microbiology 6, 674.

Salk, K.R., Ostrom, N.E., 2019. Nitrous oxide in the Great Lakes: insights from two trophic extremes. Biogeochemistry 144, 233-243.

Shaaban, M., Wu, Y., Khalid, M.S., Peng, Q.A., Xu, X., Wu, L., Younas, A., Bashir, S., Mo, Y., Lin, S., Zafar-Ul-Hye, M., Abid, M., Hu, R., 2018. Reduction in soil N_2O emissions by pH manipulation and enhanced *nos*Z gene transcription under different water regimes. Environmental Pollution 235, 625-631.

Small, G.E., Cotner, J.B., Finlay, J.C., Stark, R.A., Sterner, R.W., 2014. Nitrogen transformations at the sediment–water interface across redox gradients in the Laurentian Great Lakes. Hydrobiologia 731, 95-108.

Song, K., Kang, H., Zhang, L., Mitsch, W.J., 2012. Seasonal and spatial variations of denitrification and denitrifying bacterial community structure in created riverine wetlands. Ecological Engineering 38, 130-134.

Song, X., Ju, X., Topp, C.F.E., Rees, R.M., 2019. Oxygen regulates nitrous oxide production directly in agricultural soils. Environmental Science & Technology 53, 12539-12547.

Tian, H., Xu, R., Canadell, J.G., Thompson, R.L., Winiwarter, W., Suntharalingam, P., Davidson, E.A., Ciais, P., Jackson, R.B., Janssens-Maenhout, G., Prather, M.J., Regnier, P., Pan, N., Pan, S., Peters, G.P., Shi, H., Tubiello, F.N., Zaehle, S., Zhou, F., Arneth, A., Battaglia, G., Berthet, S., Bopp, L., Bouwman, A.F., Buitenhuis, E.T., Chang, J., Chipperfield, M.P., Dangal, S.R.S., Dlugokencky, E., Elkins, J.W.,

Eyre, B.D., Fu, B., Hall, B., Ito, A., Joos, F., Krummel, P.B., Landolfi, A., Laruelle, G.G., Lauerwald, R., Li, W., Lienert, S., Maavara, T., MacLeod, M., Millet, D.B., Olin, S., Patra, P.K., Prinn, R.G., Raymond, P.A., Ruiz, D.J., van der Werf, G.R., Vuichard, N., Wang, J., Weiss, R.F., Wells, K.C., Wilson, C., Yang, J., Yao, Y., 2020. A comprehensive quantification of global nitrous oxide sources and sinks. Nature 586, 248-256.

Veraart, A.J., de Klein, J.J.M., Scheffer, M., 2011. Warming can boost denitrification disproportionately due to altered oxygen dynamics. PLoS One 6.

Wang, G., Wang, J., Xia, X., Zhang, L., Zhang, S., McDowell, W.H., Hou, L., 2018. Nitrogen removal rates in a frigid high-altitude river estimated by measuring dissolved N_2 and N_2O. Science of the Total Environment 645, 318-328.

Wang, S., Liu, C., Yeager, K.M., Wan, G., Li, J., Tao, F., Lu, Y., Liu, F., Fan, C., 2009. The spatial distribution and emission of nitrous oxide (N_2O) in a large eutrophic lake in eastern China: anthropogenic effects. Science of the Total Environment 407, 3330-3337.

Weiss, R.F., 1970. The solubility of nitrogen, oxygen and argon in water and seawater. Deep Sea Research and Oceanographic Abstracts 17, 721-735.

Weiss, R.F., Price, B.A., 1980. Nitrous-oxide solubility in water and seawater. Marine Chemistry 8, 347-359.

Wenk, C.B., Frame, C.H., Koba, K., Casciotti, K.L., Veronesi, M., Niemann, H., Schubert, C.J., Yoshida, N., Toyoda, S., Makabe, A., Zopfi, J., Lehmann, M.F., 2016. Differential N2O dynamics in two oxygen-deficient lake basins revealed by stable isotope and isotopomer distributions. Limnology and Oceanography 61, 1735-1749.

Xiao, Q., Xu, X., Zhang, M., Duan, H., Hu, Z., Wang, W., Xiao, W., Lee, X., 2019. Coregulation of nitrous oxide emissions by nitrogen and temperature in China's third largest freshwater lake (Lake Taihu). Limnology and Oceanography 64, 1070-1086.

Xu, J., Lyu, H., Xu, X., Li, Y., Li, Z., Lei, S., Bi, S., Mu, M., Du, C., Zeng, S., 2019. Dual stable isotope tracing the source and composition of POM during algae blooms in a large and shallow eutrophic lake: All contributions from algae? Ecological Indicators 102, 599-607.

Yan, X., Xu, X., Ji, M., Zhang, Z., Wang, M., Wu, S., Wang, G., Zhang, C., Liu, H., 2019. Cyanobacteria blooms: A neglected facilitator of CH_4 production in eutrophic lakes. Science of the Total Environment 651, 466-474.

Yan, X., Xu, X., Wang, M., Wang, G., Wu, S., Li, Z., Sun, H., Shi, A., Yang, Y., 2017. Climate warming and cyanobacteria blooms: Looks at their relationships from a new perspective. Water Research 125, 449-457.

Yoon, S., Nissen, S., Park, D., Sanford, R.A., Loffler, F.E., 2016. Nitrous oxide reduction kinetics distinguish bacteria harboring clade I *nosZ* from those harboring clade II *nosZ*. Applied and Environmental Microbiology 82, 3793-3800.

Zhang, W., Li, H., Xiao, Q., Jiang, S., Li, X., 2020. Surface nitrous oxide (N_2O) concentrations and fluxes from different rivers draining contrasting landscapes: Spatio-temporal variability, controls, and implications based on IPCC emission factor. Environmental Pollution 263, 114457.

Zhang, Y., Ji, G., Wang, C., Zhang, X., Xu, M., 2019. Importance of denitrification driven by the relative

abundances of microbial communities in coastal wetlands. Environmental Pollution 244, 47-54.

Zhao, S., Wang, Q., Zhou, J., Yuan, D., Zhu, G., 2018. Linking abundance and community of microbial N_2O-producers and N_2O-reducers with enzymatic N_2O production potential in a riparian zone. Science of the Total Environment 642, 1090-1099.

Zhao, S., Zhou, J., Yuan, D., Wang, W., Zhou, L., Pi, Y., Zhu, G., 2019. *Nir*S-type N_2O-producers and *nos*Z II-type N_2O-reducers determine the N_2O emission potential in farmland rhizosphere soils. Journal of Soils and Sediments 20, 461-471.

Zhao, Y., Xia, Y., Ti, C., Shan, J., Li, B., Xia, L., Yan, X., 2015. Nitrogen removal capacity of the river network in a high nitrogen loading region. Environmental Science & Technology 49, 1427-1435.

Zhou, Y., Xiao, Q., Zhou, L., Jang, K.S., Zhang, Y., Zhang, M., Lee, X., Qin, B., Brookes, J.D., Davidson, T.A., Jeppesen, E., 2020c. Are nitrous oxide emissions indirectly fueled by input of terrestrial dissolved organic nitrogen in a large eutrophic Lake Taihu, China? Science of the Total Environment 722, 138005.

Zhou, Y., Song, K., Han, R., Riya, S., Xu, X., Yeerken, S., Geng, S., Ma, Y., Terada, A., 2020a. Nonlinear response of methane release to increased trophic state levels coupled with microbial processes in shallow lakes. Environmental Pollution 265, 114919.

Zhou, Y., Suenaga, T., Qi, C., Riya, S., Hosomi, M., Terada, A., 2020c. Temperature and oxygen level determine N_2O respiration activities of heterotrophic N_2O-reducing bacteria: Biokinetic study. Biotechnology and Bioengineering.

Zhou, Y., Xu, X., Han, R., Li, L., Feng, Y., Yeerken, S., Song, K., Wang, Q., 2019. Suspended particles potentially enhance nitrous oxide (N_2O) emissions in the oxic estuarine waters of eutrophic lakes: Field and experimental evidence. Environmental Pollution 252, 1225-1234.

Zhu, L., Shi, W., Van Dam, B., Kong, L., Yu, J., Qin, B., 2020. Algal accumulation decreases sediment nitrogen removal by uncoupling nitrification-denitrification in shallow eutrophic lakes. Environmental Science & Technology 54, 6194-6201.

Table 1. Validity of the multiple stepwise regression model for N_2O emission fluxes incorporating variables of the overlying water

Season	Parameters	Equations	Variables	Adj. R^2	*P*	Signific F-test	
						F	t_1
Summer	N_2O	N_2O = 14.33(TN) – 10.45	TN	0.91	$p < 0.001$	158.86	12.6
		N_2O = 12.36(TN) + 27.99(TP) – 13.13	TN, TP	0.94	$p < 0.001$	123.95	10.8
Winter	N_2O	N_2O = 21.04(TN) – 13.44	TN	0.80	$p < 0.001$	56.11	7.49
		N_2O = 32.06(TN) – 1.79(chl-*a*) – 1.09	TN, chl-*a*	0.90	$p < 0.001$	60.65	8.76
		N_2O = 20.68(TN) – 2.04(chl-*a*) + 22.55(NO_3^--N) + 3.13	TN, chl-*a*, NO_3^--N	0.96	$p < 0.001$	112.69	6.11
Summer + Winter	N_2O	N_2O = 18.93(TN) – 13.80	TN	0.79	$p < 0.001$	110.56	10.5
		N_2O = 23.45(TN) – 0.33(chl-*a*) – 12.03	TN, chl-*a*	0.86	$p < 0.001$	74.08	12.8

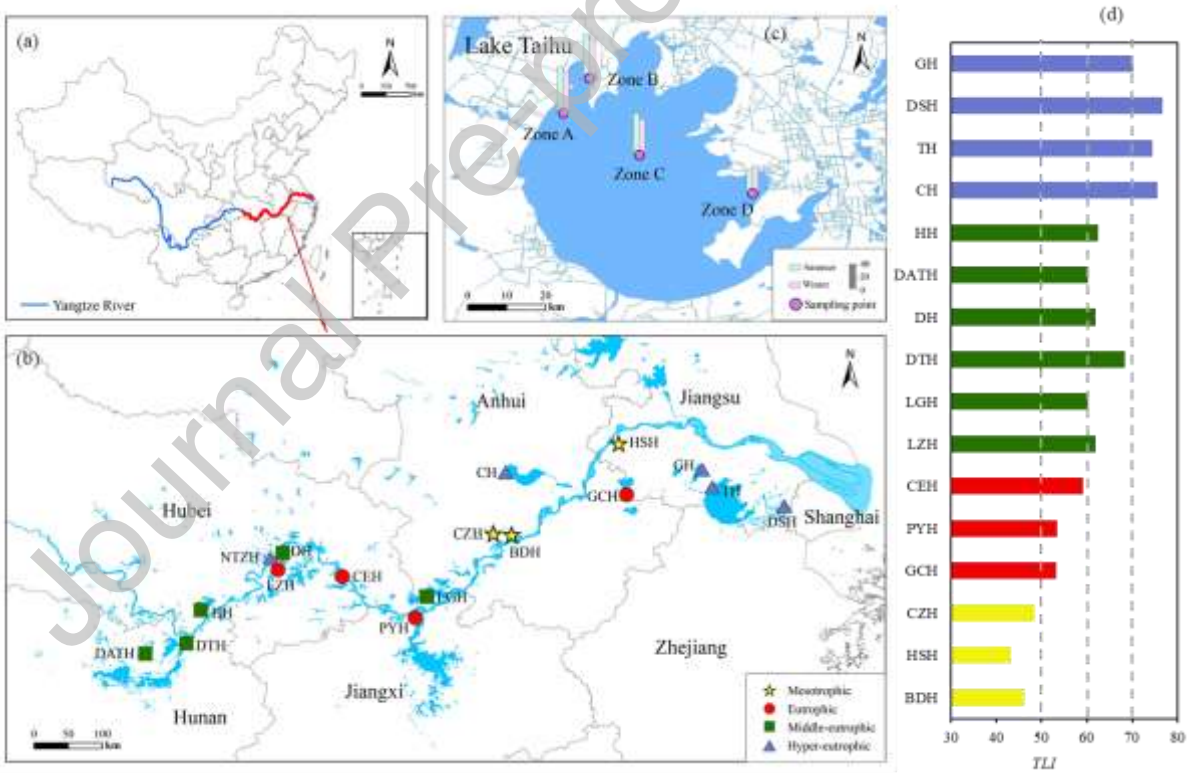

Fig. 1 Distribution of sampling sites (b) in the middle and lower reaches of the Yangtze River basin, China. Sampling sites (c) in the heavy algae-accumulated zone (Zone A and B), transitional zone (Zone C), and light algae-accumulated zone (Zone D) of Lake Tahui. The graph on the right (d) shows the *TLI* of each lake in summer. DSH: Lake Dianshang; TH: Lake Taihu; GH: Lake Gehu; GCH: Lake Gucheng; HSH:

Lake Huashen; CH: Lake Chaohu; BDH: Lake Baidang; CZH: Lake Caizi; LGH: Lake Longgan; PYH: Lake Poyang; CEH: Lake Cehu; DH: Lake Donghu; LZH; Lake Liangzi; NTZH; Lake Nantaizi; HH: Lake Honghu; DTH; Lake Dongting; DATH: Lake Datong.

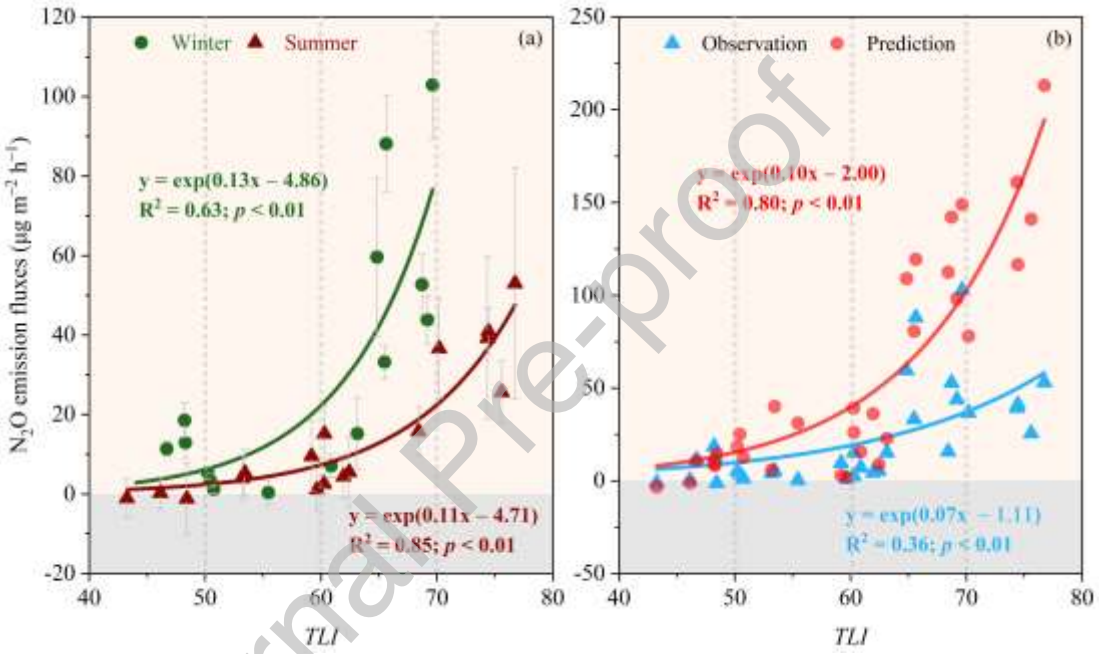

Fig. 2. Net N_2O emissions (a) in lakes of different trophic status during the winter (2017) and summer (2018). The plots (b) show the predicted N_2O emission fluxes based on the EF_{5r} of the IPCC default value (0.26%). Note that the *TLI* ranges for mesotrophic, eutrophic, middle-eutrophic, and hypereutrophic states are 40–50, 50–60, 60–70, and > 70, respectively.

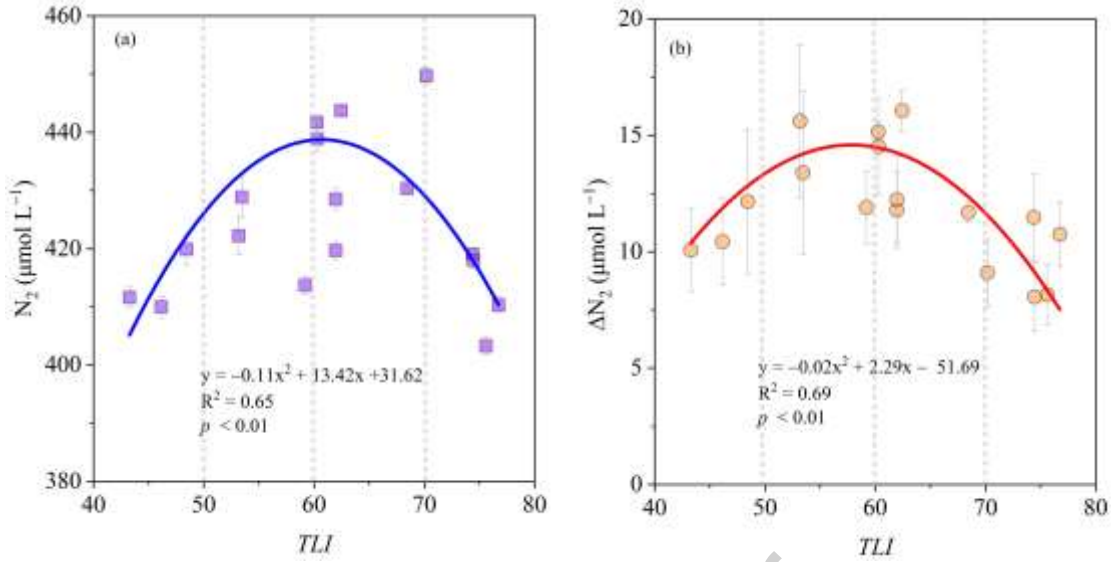

Fig. 3. The relationship between *TLI* and (a) dissolved N_2 concentration as well as (b) excess dissolved N_2 concentration (ΔN_2) in shallow lakes in summer (2018). Note that the *TLI* ranges for mesotrophic, eutrophic, middle-eutrophic, and hypereutrophic states are 40–50, 50–60, 60–70, and > 70, respectively.

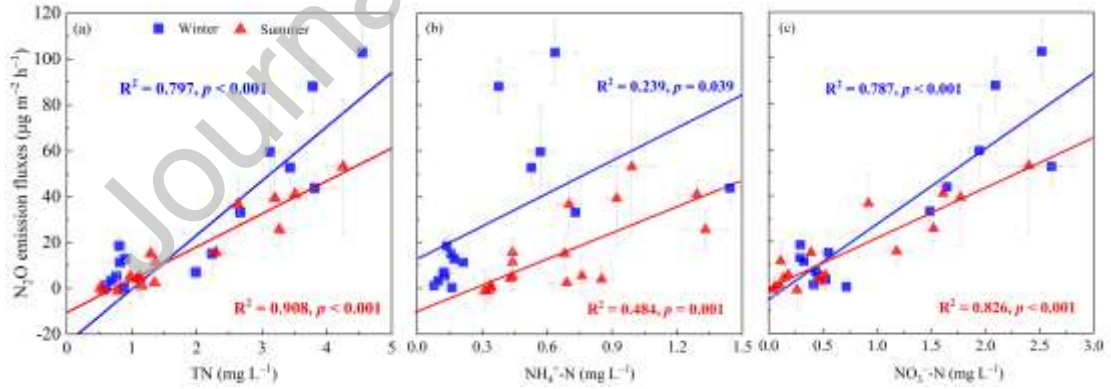

Fig. 4. Relationship between net N_2O emission fluxes and TN (a), NH_4^+-N (b), and NO_3^--N (c) in winter (2017) and summer (2018) of shallow lakes.

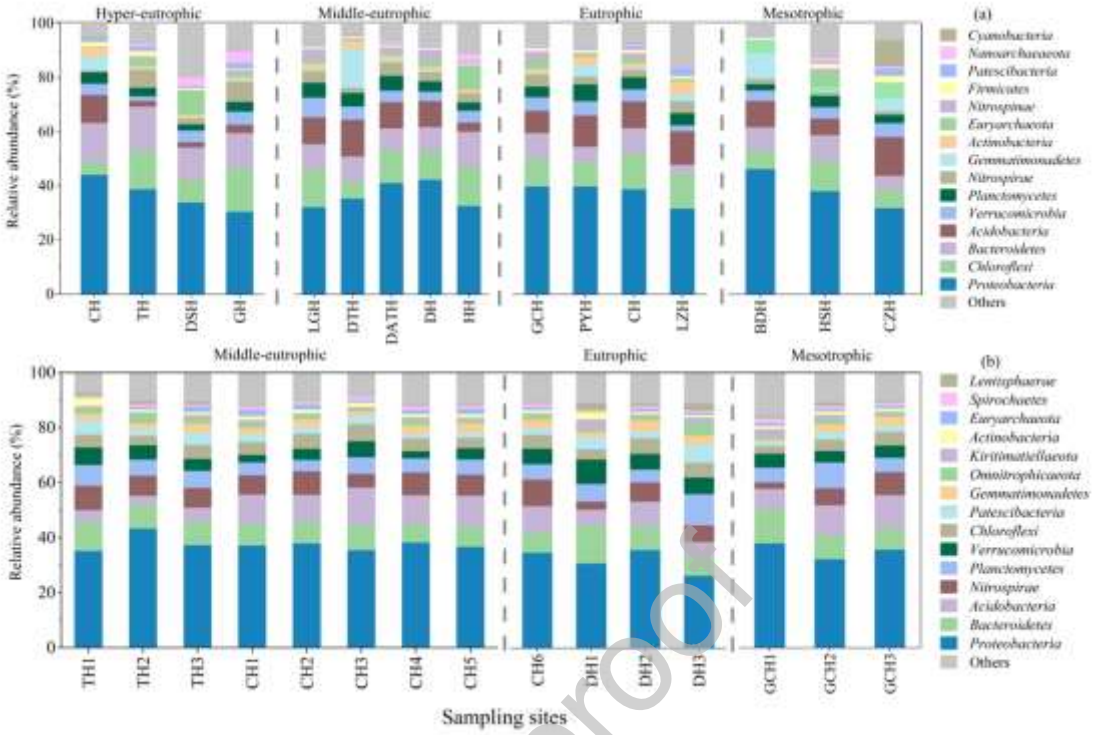

Fig. 5. Relative abundances of 16S rRNA gene-based microbial taxa for each sample at the phylum level in (a) summer (2018) and (b) winter (2017). The 15 most abundant phyla are shown.

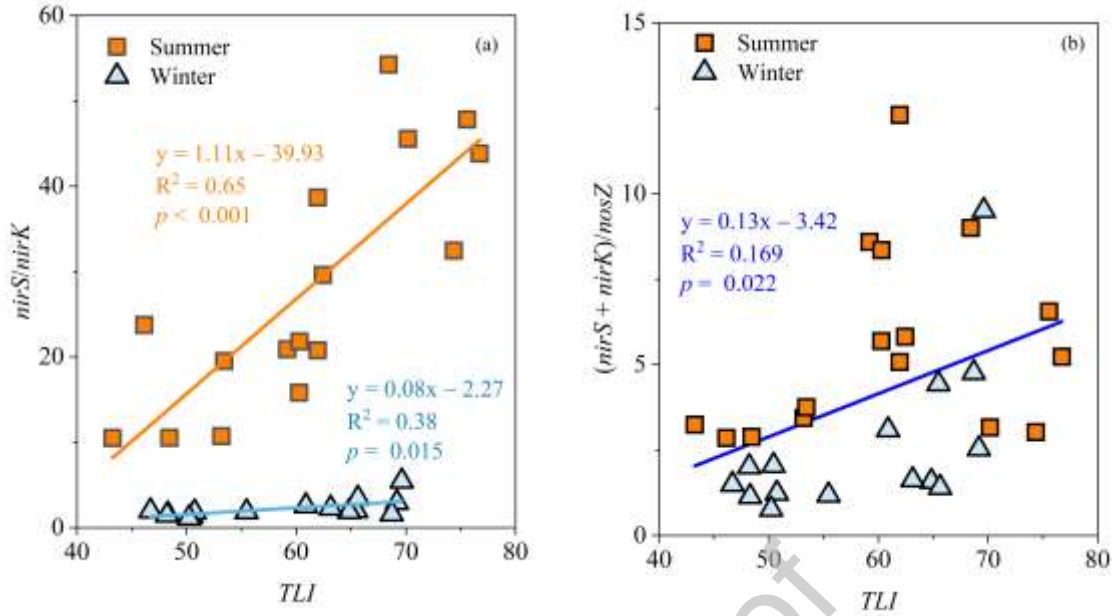

Fig. 6. The relationship between *TLI* and ratio of (a) *nirS*/*nirK* as well as (b) (*nirS* + *nirK*)/*nosZ*.

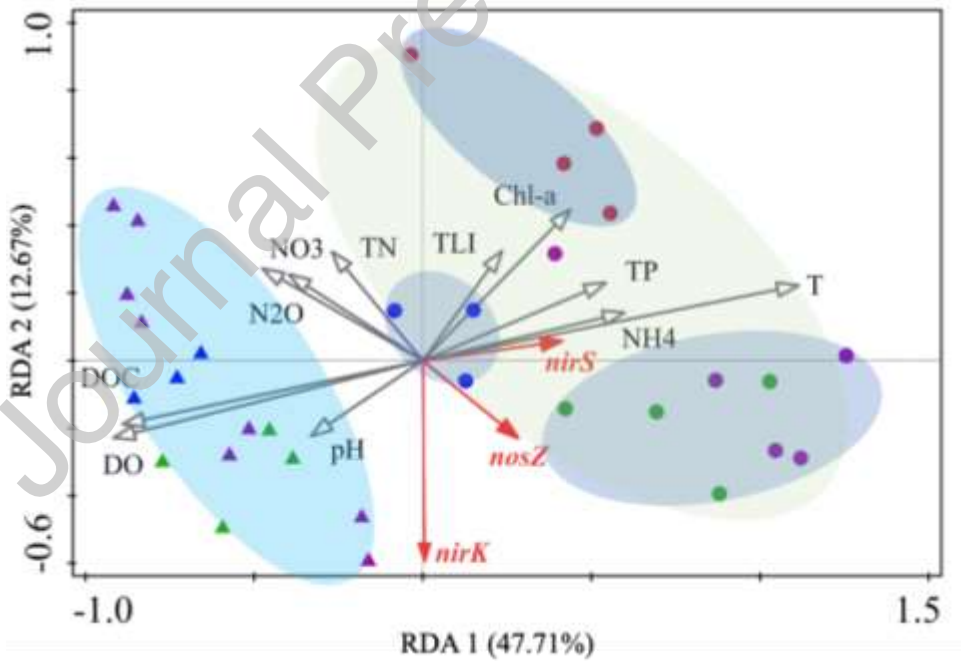

Fig. 7 Redundancy analysis (RDA) biplots of gene abundances and their relationship with environmental factors. The circle and triangle points correspond to samples taken in summer and winter, respectively. The trophic states of mesotrophic, eutrophic, middle-eutrophic, and hyper-eutrophic are represented by green, blue, violet, and red points, respectively.

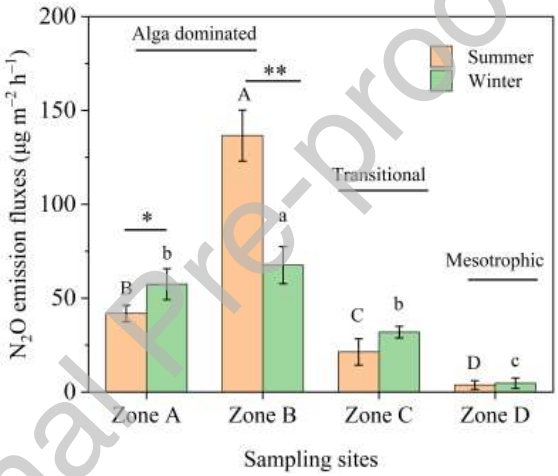

Fig. 8. Seasonal N_2O emission fluxes in heavy algae-accumulated (Zones A and B), transitional (Zone C), and light algae-accumulated (Zone D) zones in Lake Taihu. Significant differences were performed at the *$p < 0.05$ and **$p < 0.01$ levels.